PROJECT FINAL REPORT

Publishable summary

Version 1.1 – 31 July 2013

Grant Agreement number: 241270

Project acronym: E^2PHEST^2US

Project title: Enhanced Energy Production of Heat and Electricity by a combined Solar Thermionic-Thermoelectric Unit System

Project website address: www.ephestus.eu

Contents

1 Executive summary

The E^2PHEST^{2}US (Enhanced Energy Production of Heat and Electricity by a combined Solar Thermionic-Thermoelectric Unit System) project aims to design and realize innovative and scalable components for solar concentrating systems that generate both electricity and heat and work efficiently at high temperatures (800-1000°C).

The proposed concept includes the design, realization and testing of several new component technologies. A high-temperature receiver was developed to provide the heat input to the converter unit. A new-concept conversion module (CM) has been developed for electrical and thermal energy production, based on thermionic and thermoelectric direct converters, thermally combined in series to increase the efficiency. A heat recovery system was designed to collect waste heat (standard efficiency of 65%) and provide it as an additional energy product (cogeneration).

An innovative cable for fluid and electricity transport was designed, realized and tested. The benefit associated to a single hybrid cable, able to carry both relatively high-temperature fluids and electricity, was characterized and demonstrated. A small-scale prototype solar system was realized to test and evaluate the real impact of the new components.

Behind this ambitious research project, started on January 1, 2010 and which the duration is 36 months, there’s a consortium made of 7 partners from 4 different Mediterranean countries (Israel, Italy, San Marino and Turkey) that all together cover the full range of activities required to implement a successful project. In fact basic research activity is assigned to internationally recognized scientific and academic entities which contribute to this project with groups having a leading role in the research fields they have developed. CNR, headed by Dr. Trucchi, participates to the project with the efforts of two Institutes, IMIP and ISTEC headed by Ms. Dr. Sciti, fully covering almost all the R&D activities regarding the innovative materials and conversion module design and realization. TAU group, headed by Prof. Kribus, is internationally known for revolutionary concentrating solar system design. TÜBİTAK MAM is a large research centre able to contribute for characterizing the performance of the developed solar materials, in addition to a solid experience in many energy recovery topics. The SMEs involved are growing hi-tech enterprises able to interpret, smooth, integrate and exploit the know-how coming from the basic research level. SHAP R&D has skills in developing and manufacturing prototype systems for energy conversion and a solid experience in collaborating with research institutions within international projects. MAYA is at present strengthening its potentials to be able to compete in hi-tech applications. A large industry as PRYSMIAN also participated the project contributing with its know-how concerning engineering of systems and, specifically, hybrid cables competence and manufacturing. The whole consortium is supported by the no-profit entity CRR that has a long experience in EC co-funded project management.

2 Summary description of project context and objectives

2.1 Project context

The E^{2}PHEST^{2}US project background addresses the renewable energy exploitation, more specifically solar energy conversion into electrical energy, having the specific purpose of realize and fabricate innovative and scalable components for CSP systems that:

- ✓ efficiently generate at the same time electric energy and heat power;
- ✓ reliably work at high temperatures (700°C÷900°C);
- ✓ recover and exploit heat at intermediate temperature.

An originally designed conversion module (CM) prototype for the production of electric and heat energy has been developed based on direct thermionic and thermoelectric direct converters, thermally combined in series to increase the efficiency with a theoretical thermal-to-electrical efficiency >30%. An innovative hybrid cable, able to carry at the same time high-temperature fluids and electricity has been designed and tested within the project lifetime. The use of advanced new materials enabled the exploitation of thermionic effect at temperatures around 700 °C ÷ 900 °C, enhancing the conversion performance of traditional thermionic systems, which traditionally required higher cathode temperatures (>1300 °C). Nevertheless, it is worth to say that thermionic stage efficiency is independent of anode temperatures up to temperatures <400 °C, where a thermoelectric stage can be added to exploit the thermal range down to room temperature. These complementary properties allowed the development of an integrated system, thus making the best use of thermal energy generated at different temperatures and achieving a better value of total efficiency. The geometrical and operational versatility of the conversion module prototype unit makes it suitable for future use in a wide range of CSP systems (parabolic troughs, solar towers, dish, Fresnel lenses). A single CM prototype could vary its output ranging from few W up to several kW, owing to its up-scalability (size, technology and manufacture), increased also by the fact that the modules can be arranged in arrays.

The small-scale prototype system allowed the evaluation of the performance in comparison with similar systems in terms of output power, production cost, duration and reliability.

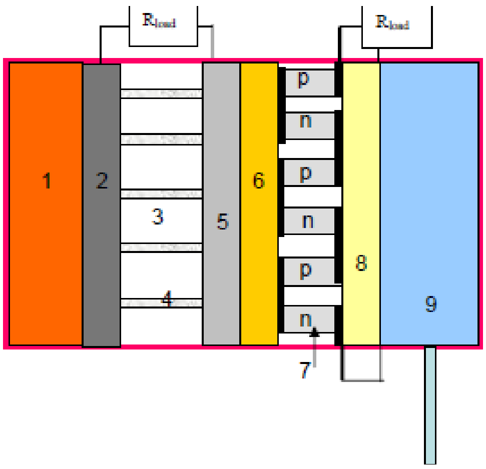

1)Solar radiation receiver, transforming solar radiation energy into thermal energy (at temperature TR).

2) Thermionic emitter at high temperature, TE ≈ TR (700°C÷900 °C).

3) Inter-electrode space.

4) (Optional) Thermally insulating spacers for inter-electrode distances <10 µm.

5) Thermionic collector TC << TE.

6) Electrically insulating, thermally conductive layer (300-600°C).

7) Semiconducting thermoelectric elements and electric wirings.

8) Electrically insulating, thermally conductive layer.

9) Passive (or active) heat sinker.

Fig.1- CM Prototype design

2.2 Results

The energy conversion was based on the design and development of:

- Thermal efficient solar absorber receiver for high temperature (>700 °C). This activity was carried out by developing, characterizing and testing the proper absorber materials which were engineered ceramic materials, characterized by thermal stability operation in vacuum conditions. Solar absorbance higher than >90% has been obtained by developing a novel surface texturing treatment able to induce nano-structuring processes to enhance solar light capture. Thermal emittance values around 55% at operating temperature range have been obtained by engineering the physical properties of the ceramic materials.

- The most proper thermionic material able to work at relatively low temperature (700 – 1000 °C) has been developed (n-doped polycrystalline diamond), and deposited monolithically as a thin film by CVD on the back surface of the ceramic receiver.

- A commercial thermoelectric module has been selected, tested and integrated.

- The monolithic integration of absorber, thermionic and thermoelectric stages, and heat recovery system has been realized in a conversion module (CM).

- Solar test platform (STP), able to guarantee a high flux distribution for making a standard absorber reaching the requested operating temperatures, has been designed and built in field.

The technical requests to be satisfied are high solar concentrating ratio (400 – 1000 suns), high energy flux homogeneously on the absorber surface to guarantee high temperature (700°C ÷ 900 °C).

- The chosen configuration of STP has been matched with the CM geometrical specifications and successively the CM has been integrated to form the solar prototype system.
- A control unit and acquisition system has been developed and integrated with the STP and CM
- Hybrid cables carrying electricity and fluids to allow an efficient and compact cogeneration. The technological development of hybrid cables was specifically addressed to issues related to fluid temperatures up to 120 °C. This activity included the optimization of both conductor and polymeric insulation and sheath. The stability and durability of cable has been verified, and the integration in the STP within the whole prototype solar system has been performed.
- Development of three CM version: CM-Alpha (“naked” CM composed by active components and strictly necessary elements), CM-Beta (CM combined to an additional pumping system), and CM-Gamma (encapsulated CM, developed by performing a specific vacuum encapsulation of conversion module) . All the components of CMs have been properly optimized, assembled and, in the case of CM-Gamma, encapsulated under *vacuum*, with a special designed procedure.
- Fabrication of a prototype pilot system for the energy conversion of concentrated solar radiation: Installation of the CM-Beta and Gamma versions at the focus of the STP parabolic concentrator, electrical connection and automatic computer-driven control of the whole integrated system.

- Power and electrical test measurements of CM-Alpha version under a high-flux solar simulator.
- Power and electrical test measurements of encapsulated CM (Gamma version) at the solar test platform (STP) under outdoor conditions.

The CM (gamma version), integrated in the STP at the focal point of the parabolic concentrator, at the SHAP headquarters in Castel Romano - Rome (ITALY), is shown in fig. 2.

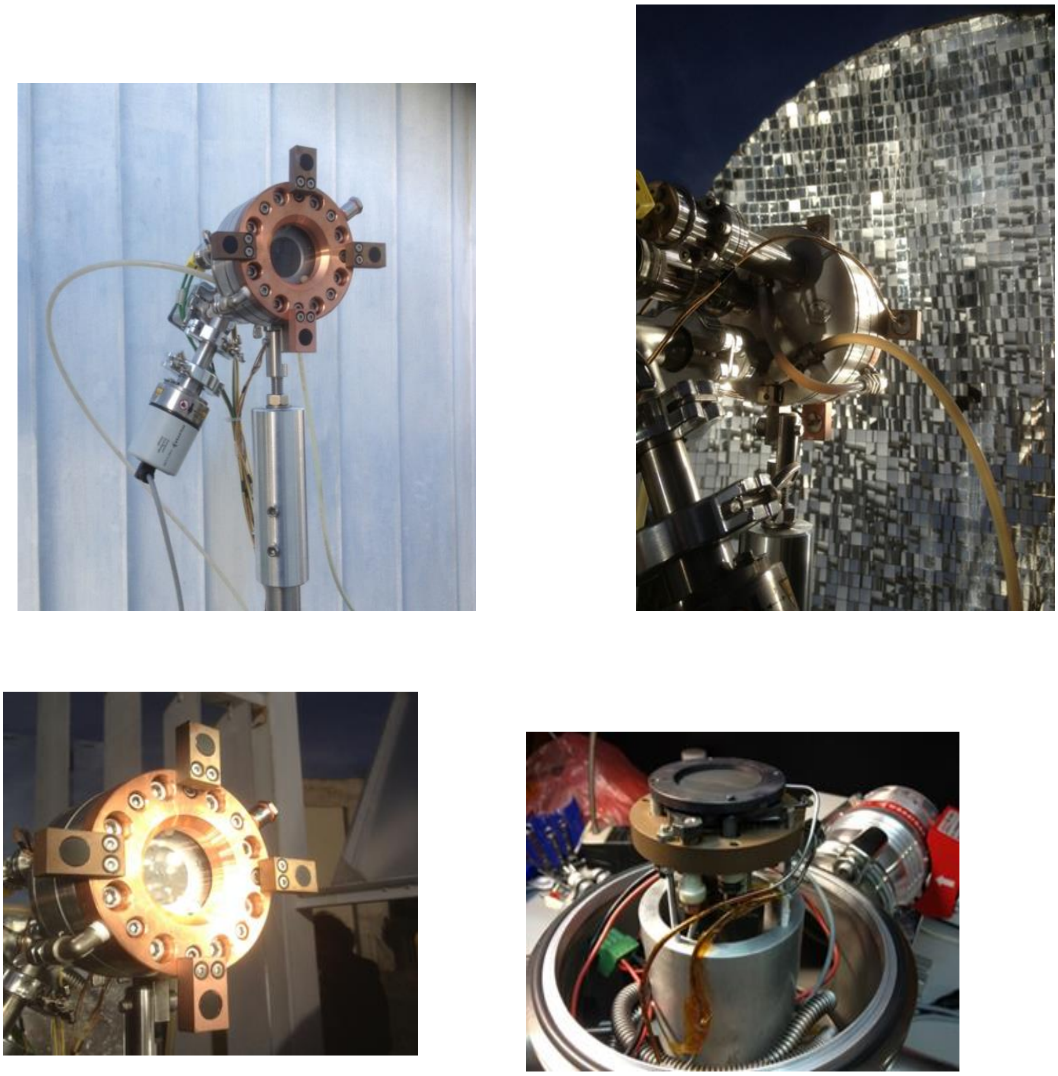

Fig. 2. The CM (gamma), integrated in STP at the focal point of the parabolic concentrator (front and rear view), located at SHAP headquarters in Castel Romano-Roma.

2.3 CM Performance

The testing activity was split into three sub-activities: lab-level characterization of the integrated thermionic-thermoelectric conversion stages with a method based on thermal flow; lab-level CM performance characterization under high-flux solar simulator in a vacuum chamber; outdoor CM performance evaluation under STP.

As expected, in these experiments the efficiency of the system has been found to be strictly related to the temperature reached by the absorber ceramic material and also to the vacuum operating level.

The first characterization activity provided thermal-to-electric conversion efficiency close to 6% that decreases to 0.2% for the CM under real irradiation testing. Generally speaking, although it is necessary to acknowledge the extreme novelty of the work performed, the values of power and current measured in the CM system are quite low and not completely satisfactory, if compared to our prediction in the DoW. Thermal conversion efficiency was evaluated to be close to 60%, an optimal value for allowing cogeneration.

The strict dependence of thermionic and thermoelectric emission processes, from vacuum level and receiver/emitter temperature has considerable influence on the final results, since, in real operative experimental conditions of manufactured prototype CM (gamma version), installed and positioned in the field, and subjected to specific tests, many of the crucial parameters for the attainment of optimal values of thermionic emission (eg. Temperature ≥700 °C) have not been achieved, owing to hard and complex technological problems and drawbacks, very difficult to solve in the short term and in the limited time available, at the very end of the Project.

In the encapsulated Conversion Module, specifically, many parameters are very sensitive and difficult to control and optimize, since we are dealing with a multi-component and complex prototype system, with innovative materials and processes, all difficult to control strictly, both as regards the vacuum, temperature and other properties. All these parameters are linked to the performance of the innovative materials, in particular, absorption of light, texture, stability of the coatings (adhesion), stable H-terminated n-doped diamond films (thermionic emitter material), appropriate work function difference between the cathode and anode, various seals and electric passing–through, low and not sufficient level of temperature reached by the STP at the focal point.

At this point we can clearly see some weaknesses, which can be easily addressed and solved with further research/process optimization:

- low work function difference between diamond emitter (cathode) and molybdenum receiver (anode);
- probable presence of space charge effect (further tailoring of the inter-electrode region);
- low energy fluence value at the focal point of the Solar Test Platform;
- insufficient value of temperature reached by the absorber material in the encapsulated CM.

Solutions require further research/optimization, of both fundamental and technological type, to the extent that you want to achieve substantial improvements of the whole system

- Improve material properties and related treatments (complex ceramic receiver, surface nano-texturing, diamond quality, doping and H-termination, adhesion, higher difference of work function (anode-cathode) by cesium treatment of Mo surface, minimizing inter-electrode distance, better quality commercial thermoelectric components.
- Strive to reach the maximum obtainable value of vacuum controlling the whole system, undesired outgassing under heating, optimum sealing materials, getters quality.
- Introduce mechanical spacers to reduce gap width, avoiding space charge-effects
- The energy fluence at the STP should be verified during the summer season, in order to have a better weather stability and a more reliable statistical analysis, and some STP components, which are not working optimally, possibly substituted.

It is important to emphasize that E^{2}PHEST^{2}US has been a project with the greatest scientific and technological ambitions, since it has tried to take advantage of two well-known physical phenomena but rarely exploited for solar applications, such as thermoelectric and thermionic effect, to be able to use the energy of the sun, properly concentrated at least 400 times, to generate electricity and useful energy, combining them in an integrated, new designed prototype device, like the conversion module CM.

This goal has been pursued by constructing a new concept, conversion module (CM) integrated in a solar platform (STP), apt to concentrate the light in a focal point, where is placed the absorber / emitter device, in which the temperature is elevated up to the values of the lower limit (> 700°C) to obtain a good thermionic emission, in vacuum, collected by a lower work-function cathode, placed at low temperature, in turn integrated electrode of a thermoelectric system.

The results obtained are technologically and scientifically very significant, in terms of materials, prototypes and innovative processes; some limitations, however, were found on the real yield of the two combined processes, but many of these weaknesses can be relatively easily overcome in a near future with an appropriate additional research & development phase, which can integrate the present results.

The scientific and technological achievements, obtained during the whole project, are of great relevance and led also to the submission of 3 patents, in addition to successful presentations at International Conferences.

3 Description of the main S&T results/foregrounds

3.1 Project activities, at a glance

3.1.1 The conversion module (CM) by CNR

Starting from the schematic draw of our CM structure (Fig. 3), the research work, performed during the Project time, was aimed at the study, design and manufacture, in series or in parallel, of the individual components of the module itself. As it can be clearly seen, the most important part of the CM is the definition of a complex structure, constituted by a radiation absorber, a thermionic emitter cathode, an anode (or collector) and, in series, a thermoelectric converter.

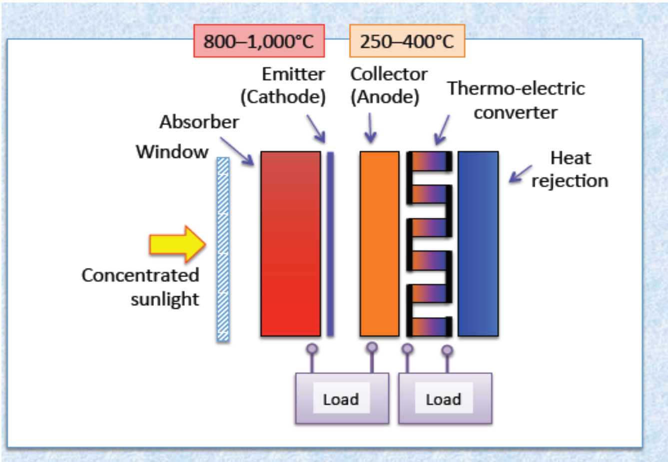

Fig. 3 - Conversion module (CM) basic structure

3.1.2 The solar test platform (STP) by SHAP

The study, design and development of a concentrating solar test platform (STP) started contemporarily to tasks concerning the conversion module (CM) that was defining materials and technological/physical specifications outputs; such a STP has been installed outdoor at SHAP headquarters, in Castel Romano (Rome, IT). The CM and STP activities, obviously, proceeded in parallel, while guidelines have been drafted to optimize and characterize materials in operating conditions. A detailed design of the STP, in coordination with the plant control and data acquisition system, has been realized in parallel to the CM materials definition and development during the first period of the Project.

Associated to this activity, a great effort has been also devoted to the optimization of the concentrating solar system in terms of mechanics, optics, tracking system, wirings and integrated circuits. The full operation of the platform, in particular focus positioning and sun tracking, is controlled by a complex automated system.

A scheme of the selected configuration for the STP is reported below (Fig. 4).

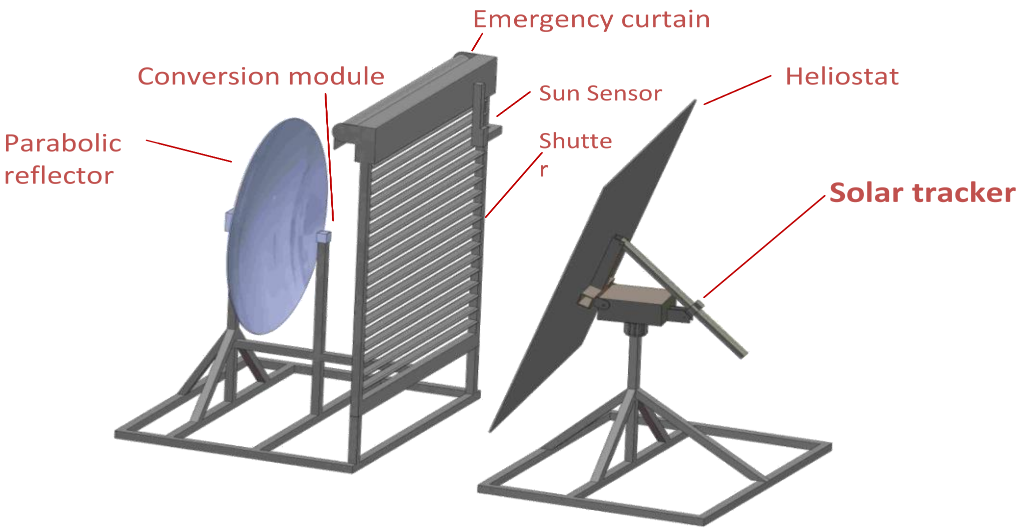

Fig. 4- A scheme of the solar platform showing the position of the conversion module (CM), placed between the heliostat and the parabolic concentrator.

3.1.3 The high flux solar simulator testing at Tel Aviv University (TAU)

Solar simulator at Tel Aviv University (TAU), schematically shown in Fig. 5, is powered by a 4 kW Xenon lamp and equipped by a concentrating reflector and a x,y,z moving stage; it works with an average energy flux of 450 kW/cm^2 (i.e. 450 mean suns) on a spot with 35 mm diameter and has been used for testing of the first prepared CM prototype (identified as α or "naked" version).

This step is mostly relevant since, with this apparatus, it is possible to independently vary different experimental parameters such as temperature, radiation flux concentration, vacuum, etc. and properly evaluate their influence on the prepared components and materials, before proceeding with the assembly of the in vacuum or encapsulated prototype.

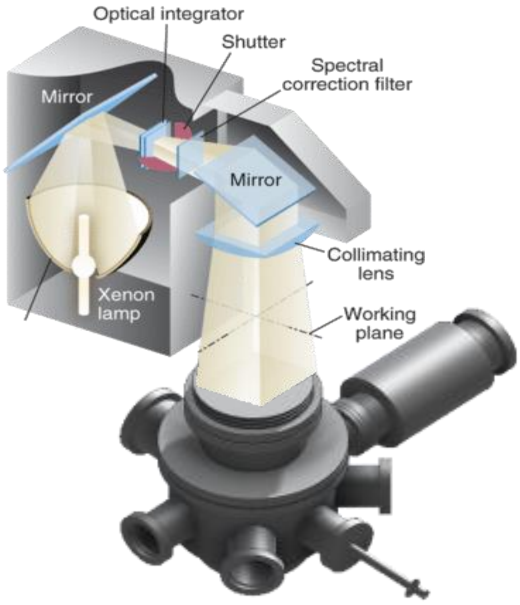

Fig. 5. The solar simulator at TAU.

3.1.4 The hybrid cable by Prysmian

A new designed hybrid cable (Fig. 6), carrying both electricity and fluids, has been fabricated and tested by Prysmian. The technological development of this hybrid cables came across mainly issues related to high temperature. This activity included the optimization of both conductor and polymeric insulation sheath. Moreover, hybrid cables integration in the STP has been established and stability and durability tests have been performed accurately. The technology and know-how (patent pending at the moment of this document drafting) have developed the basis for the final integration of cable within the prototype solar system.

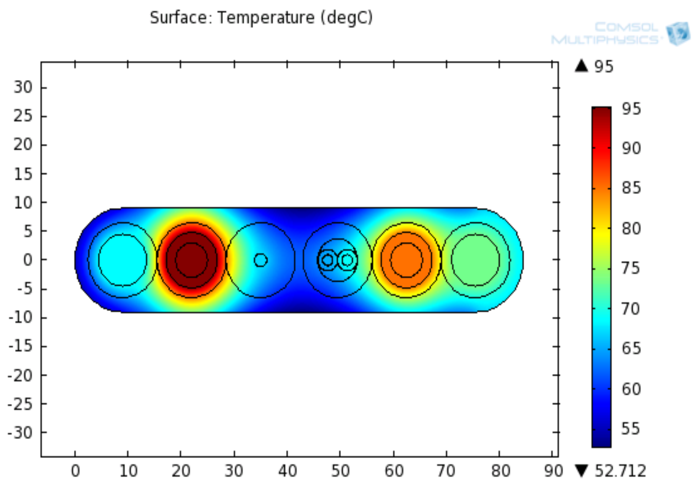

Fig. 6. The hybrid cable section, with mapped simulation of expected temperature.

3.1.5 The CM, Beta and Gamma version, outdoor installed in the solar test platform (STP) by CNR and SHAP

Following pictures, Fig 7 and Fig. 8, actually represent the end of the project E^{2}PHEST^{2}US. In Fig. 7, it is presented the installation and integration of the CM beta version in the solar test platform, still assisted by an external pumping vacuum system directly connected to the module.

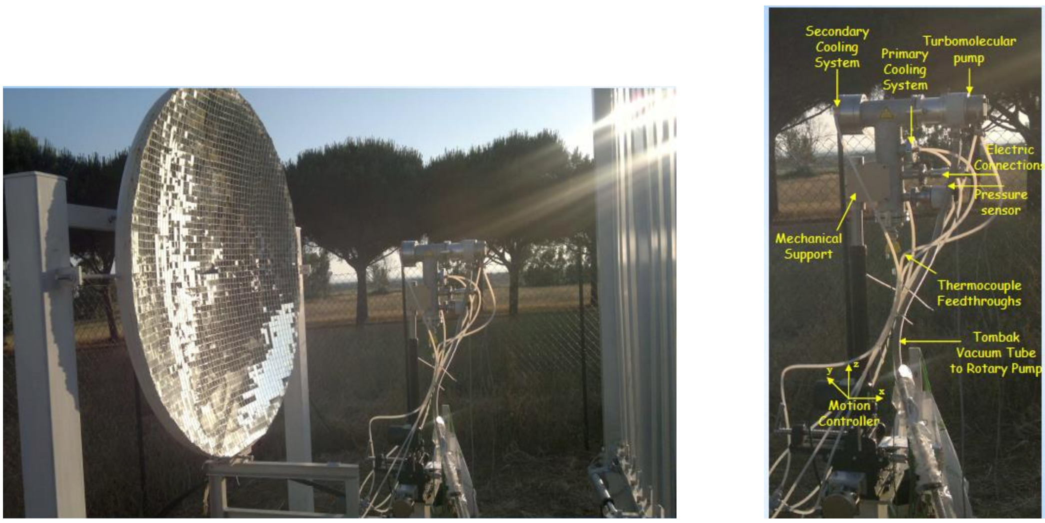

Fig 7. The CM (β) positioned at the focus of the parabola (*left*); the CM with the vacuum pump behind and the x,y,z motor system at the basis of the whole apparatus (*right*)

Fig 8a,b,c presents the final prototype version of the conversion module CM, in the gamma version, encapsulated under vacuum, and installed in the field, at the STP, built by SHAP, at Castel Romano – Rome.

Finally, the whole integrated system (CM module and STP), including all system securities, is automatically controlled by computers, with development of programs performed within NI Labview software environment, ad hoc specifically prepared.

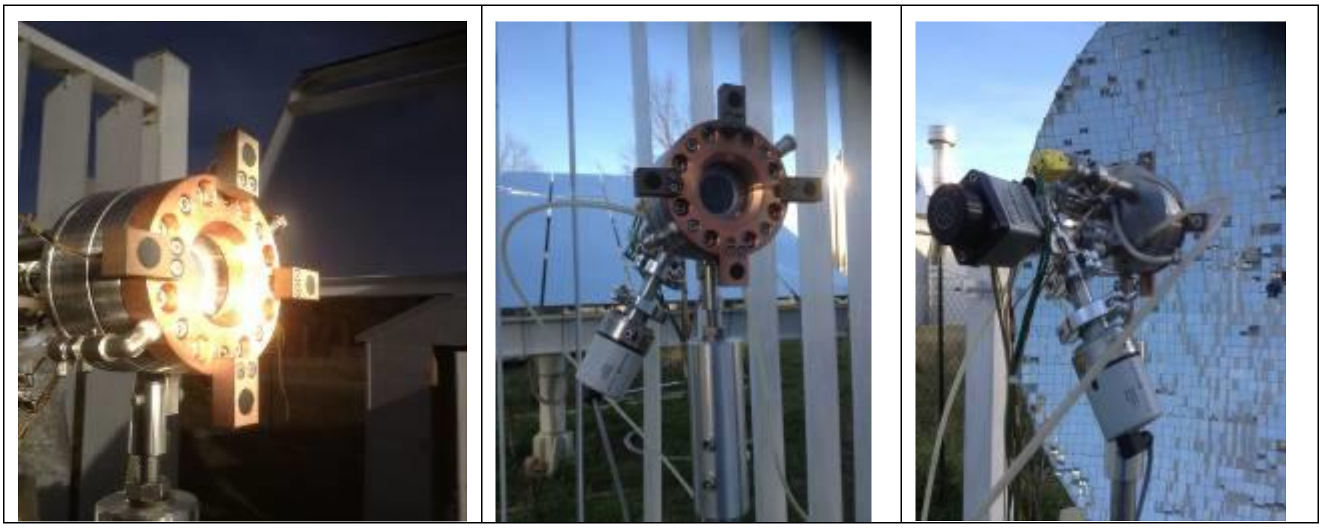

Fig. 8. The encapsulated CM, the gamma version (a, left); front view of CM (gamma) integrated in the STP at the focal point of the parabolic mirror (b, centre) and rear view (c, right) located at SHAP headquarters in Castel Romano-Rome

3.2 The steps of the Project

3.2.1 Investigation, selection and preparation of the absorbing materials composing the solar radiation receiver

The most advanced material systems for heat collection at high temperature are constituted by high refractory composites, ceramic based material (Carbides, nitrides and borides) and the "so-called" cer-mets (very high absorbing metal-dielectric composites consisting of fine metal particles randomly dispersed in a dielectric or ceramic matrix, coated by an antireflection layer or properly treated at surface). Current available commercial coatings do not have enough stability and performance necessary to work in air at high operating temperatures (>500 °C). The proper materials should have a low diffusion coefficient at high temperature and should be chemically stable in front of degradation caused by oxidation or secondary phase formation, over long operative time at elevated temperature.

Absorber material efficiency is mainly defined by two coefficients: α, the absorbance, and ε, the emittance. The more α approaches unit and ε tends to zero, larger is the radiation energy absorbed and converted into heat, independently from a subsequent exploitation by pure thermal or electrical conversion processes. Evidently, large α/ε ratios result in small produced energy costs. The chosen solution was to produce bulk absorbers in which high spectral selectivity is already an intrinsic material property, also characterized by elevated melting point and large negative Gibbs formation free energy. The ideal absorber should have the following properties, in order of importance:

- Melting point higher than operative temperatures (800 – 1000 °C).
- Mechanical resistance at high temperatures.
- Critical thermal shock resistance compatible with the concentrated solar irradiation to face possible operation temperature variations (caused, for example, by variations of weather condition, clouds, sun-tracking errors, etc.).
- Solar radiation absorbance as high as possible to increase concentrated radiation-to-thermal energy conversion efficiency.
- Low blackbody radiation emission at operative temperature to minimize energy losses and avoid heating of elements surrounding the absorber.
- Thermal expansion coefficient and lattice compatibility matched to that of TI active emitter material.
- Electrical resistivity as low as possible to provide TI emitter a sufficient electron refilling.
- Not reactive to oxygen if exposed to atmospheric conditions at high temperatures.

A complex decision procedure was necessary to examine the best properties of different candidates, prepared by sintering process by CNR-ISTEC. The most suitable materials have been chosen according to previously listed properties.

Table 1 below reports a synthetic prospect of the properties of the materials to be employed as absorbers in E^2PHEST^2US project. It is worth to notice that thermal critical temperature of the ceramic materials is measured by suddenly immerging them at a determined temperature into room-temperature water. Actually the critical temperature in our system, characterized by a higher thermal inertia, will be increased of some hundreds Celsius degrees: in other words, although some materials do not show high critical temperature (i.e. 133 °C of HCM-5), sudden illumination variations in our application will not imply breaks or degradation to the material structure.

Table 1: Properties of the materials developed by CNR-ISTEC and of the other materials taken into account for the absorber

Material	**Acronym**	T_M (°C)	ρ (g·cm^{-3})	*dTc* (K)	K_{Ic} (MPa·m$^{1/2}$)	σ (MPa)			K_{Th} (W·m^{-1}·K^{-1})		
						@ RT	**@ 1000 °C**	**@ 1300 °C**	**@ RT**	**@ 500 °C**	**@ 1000 °C**
HfC + 5% $MoSi_2$	**HCM-5**	3880*	11.17	~133 **	3.62 ± 0.13	465 ±45	-	~408	~23	~23	~35
HfC + 30% $MoSi_2$	**HCM-30**	3880*	11.17	~124 **	~3.43	~383	-	~350	~23	~23	~33
SiC	**S**	3008*	2.09	125*	4.6*	675*	-	-	110*	65*	45*
SiC + 6% Al_2O_3 + 4% Y_2O_3	**SAY**	~3000	3.23	317**	2.97 ± 0.15	746 ± 46	528 ± 53	159 ± 7	-	-	-
(SiC + 6% Al_2O_3 + 4% Y_2O_3) + 30%vol $MoSi_2$	**SAYM-30**	~3000	4.05	352**	4.8 ± 0.2	824 ± 33	654 ± 4	162 ± 3	-	-	-
(55%vol AlN + 15vol% SiC + 30vol% $MoSi_2$) + 2wt% Y_2O_3	**ASMY-30**	-	3.76	400	4.00 ± 0.02	411 ± 16	384 ± 51	432 ± 56	27.9	17.9	14.5
Molybdenum	**Mo**	2863	10.28	-	16	329	-	-	138	-	-
Tungsten	**W**	3422	19.25	-	28.5	610	-	-	173	-	-
Pyrolitic Graphite	**C**	3650 (sublimation)	2.18 - 2.22	-	1.5	120	-	-	80 - 240	-	-

TM = Melting Point, ρ = Bulk Density, dTc = Thermal Shock Resistance, HV = Vickers Hardness, KIc = Fracture Toughness, σ = Flexural Strength, KTh = Thermal Conductivity

*Literature data, ** Calculated data

Ceramic samples sintered by CNR-ISTEC

The ceramic plates have been prepared maintaining a “rough” and a polished (“flat”) surface, in order to obtain a qualification of surface morphology independent from materials not negligible intrinsic porosity and consequently correlated only to the material properties (i.e. absorption coefficient).

Optical characterization (absorbance measurements)

The optical characterization of absorber materials has been performed both on rough and polished surfaces of each sample, to evaluate the influence and relevance of surface morphology on radiation absorbance, in the UV/Visible/IR range.

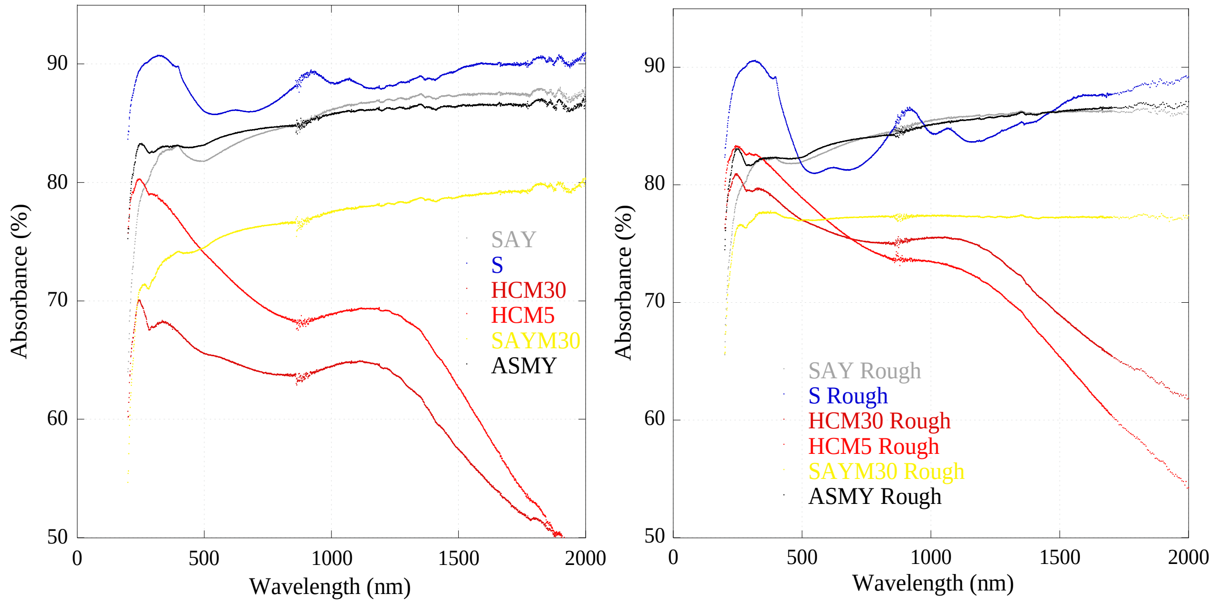

Fig. 9. Absorbance spectra for a) flat surface and b) rough surface. The signal noise from 860 to 900 nm is due to the internal exchange of the spectrometer detectors (UV-IR to UV-Visible).

Fig. 9 reports the absorbance of flat and rough surfaces for the sintered ceramic samples. It can be qualitatively observed that the highest absorbance is shown by the pure silicon carbide (set S) materials, even if SAY and ASMY achieve values comparable among them and high enough to guarantee good solar radiation absorption.

Intermediate values have been obtained by SAYM30; the lowest has been shown by hafnium carbide-based materials (HCM5 and HCM30). Specifically, among hafnium-carbide (HfC) samples, although the absorbance spectra have similar shape, higher absorbance has been achieved for HCM5: such a sample differs from HCM30 for a lower percentage of $MoSi_2$ content (just 5% against 30%). The same comparative results among different samples remain valid for rough surfaces, which generally show higher absorbance than the flat ones, owing to the geometrically-induced capability of entrapping the radiation (or limiting its reflection).

With the aim to evaluate efficiency of each absorbing material with respect to the spectral energy content of the solar radiation, absorbed solar power (W_{abs}*) has been defined, per wavelength unit, as the product between the absorbance and the incident solar spectral irradiance. This parameter, is shown for each flat surface of the developed ceramic materials in Fig. 10, as a function of radiation wavelength.

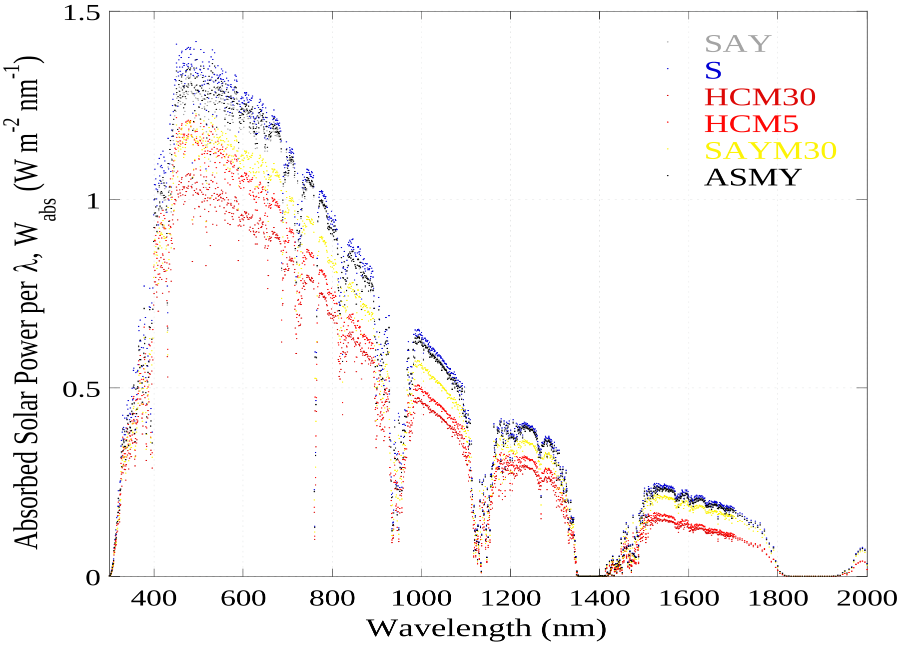

Fig. 10. Absorbed solar radiation power per wavelength unit, for the flat surface of the developed ceramic samples.

The "solar absorbance" (α) is the absorption efficiency of a material with respect to the total solar radiation power (eq.):

$$\alpha = \left(\int_{\lambda=200nm}^{\lambda=2000nm} A(\lambda) W_{solar}(\lambda) d\lambda\right) / \left(\int_{\lambda=200nm}^{\lambda=2000nm} W_{solar}(\lambda) d\lambda\right) \qquad (1.2)$$

Fig. 11 reports schematically the efficiency values of each ceramic material where solar absorbance has been pointed out both for flat and rough surface.

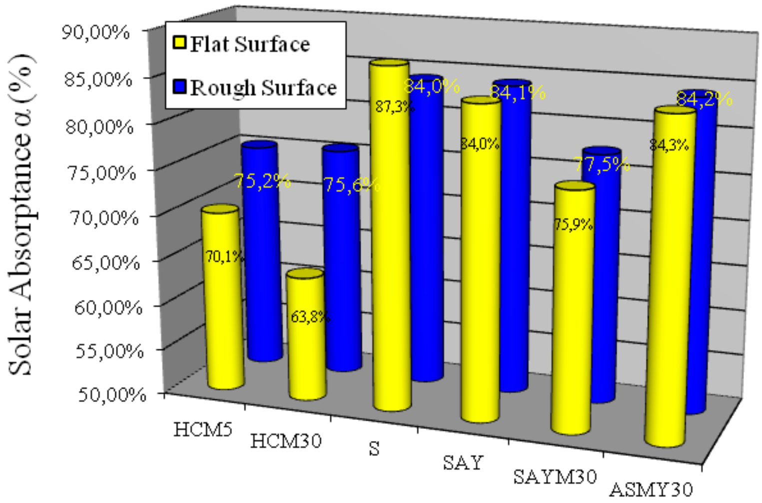

Fig. 11 - Solar absrbance α for flat and rough surface of all examined samples.

Table 2 summarize reported data concerning analysed materials in terms of absorption capability. In order to give an immediate comparison, absorption properties have been resumed by synthetic marks (*: decent, **: good, ***: excellent).

Sample Name	Material	Mean Roughness of flat surface (μm)	α (%)	Solar Absorption Efficiency
HCM-5	HfC + 5% $MoSi_2$	0.10	70.10	**
HCM-30	HfC + 30% $MoSi_2$	0.04	63.80	*
S	SiC	0.56	87.25	***
SAY	SiC + 6% Al_2O_3 + 4% Y_2O_3	0.03	84.00	***
SAYM-30	(SiC + 6% Al_2O_3 + 4% Y_2O_3) + 30%vol $MoSi_2$	0.03	75.94	**
ASMY-30	(55%vol AlN + 15vol% SiC + 30vol% $MoSi_2$) + 2wt% Y_2O_3	0.10	84.33	***
W	W (99.999% purity)	0.10	59.48	*
Mo	Mo (99.999% purity)	0.10	51.17	*
C	Pyrolitic Graphite (99.999% purity)	1	77.10	**

Table 2. Solar absorption efficiency of the sintered ceramic materials, to which has been assigned a mark; (*) identifies the lowest value, while (***) the highest value.

On the basis of previous discussion, samples can be distinguished in three different clusters:

1. **Hafnium Carbide-based samples** *(HCM5, HCM30)*: characterized by the lowest absorption efficiency,; HCM5 (5% $MoSi_2$ inclusion) achieves better performance than HCM-30 (30% $MoSi_2$ inclusion) concerning the flat surface, while absorption efficiency of rough surfaces is approximately the same (about 75%). Two considerations come out: $MoSi_2$ content decreases material absorption capacity, although balanced by disordered surface morphology that enables better light trapping.
2. **Silicon Carbide-based samples** *(S, SAY, SAYM-30)*: pure silicon carbide (S) is the most efficient among analysed materials although it has to be considered that the high specific absorption coefficient α has been demonstrated for a flat side with an average surface roughness of 0,56 µm, probably due to a slightly porous microstructure. SAY achieves good efficiency values, which are comparable to pure SiC for its rough surface (disordered morphology) and are far larger than those of SAYM-30, both for flat and rough surfaces. SAY and SAYM-30 differ for $MoSi_2$ concentration (0% and 30%, respectively): this represents another evidence of MoSi2 detrimental effect on the absorption properties.
3. **Aluminium Nitride-based samples** *(ASMY-30)*: it has a high absorbance (84%) both for rough and for flat surface.

Electric Characterization by CNR-IMIP

Electric properties of ceramic samples are fundamental requirements for the functionality of the absorber material in the CM. The absorber material, indeed, has to provide thermal energy as well as a sufficient refilling activity of electrons to the thermionic emitter. From an electric point of view, the radiation absorber represents a resistance in series to the thermionic emitter: its electric resistance should be as low as possible in order to not represent a bottleneck for electron emission. Such a series resistance depends obviously on the electric connection geometry and electric simulations indicated that resistivity values smaller than 5 Ω cm could be acceptable. Table 3 reports the electric resistivity of the analysed samples, evaluated by their current-to-voltage characteristics and/or by four-point-probe technique. These two techniques are complementary used as a function of the resistance range of samples. Again, in order to give an immediate comparison, absorption properties have been resumed by synthetic marks (*: decent, **: good, ***: excellent).

Sample Name	Material	Electric Resistivity (Ω cm)	Electric Performance
HCM-5	HfC + 5% $MoSi_2$	$(1.66 \pm 0.34)\times10^{-4}$	***
HCM-30	HfC + 30% $MoSi_2$	$(9.29 \pm 0.31)\times10^{-5}$	***
S	SiC	$(5.06 \pm 1.02)\times10^{2}$	*
SAY	SiC + 6% Al_2O_3 + 4% Y_2O_3	$(4.34 \pm 2.60)\times10^{3}$	*
SAYM-30	(SiC + 6% Al_2O_3 + 4% Y_2O_3) + 30%vol $MoSi_2$	$(2.27 \pm 0.38)\times10^{-4}$	***
ASMY-30	(55%vol AlN + 15vol% SiC + 30vol% $MoSi_2$) + 2wt% Y_2O_3	4.06 ± 2.38	**
W	W (99.999% purity)	5.28×10^{-6}	***
Mo	Mo (99.999% purity)	5.34×10^{-6}	***
C	Pyrolitic Graphite (99.999% purity)	$(2.50 \pm 0.10)\times10^{-2}$	***

Table 3. Electric resistivity and electric performance marks, evaluated for the specific absorber material functionality.

Also this time, ceramic samples can be grouped in three sets:

1. **Hafnium carbide-based samples** *(HCM5, HCM30)*: characterized by the lowest electric resistivity among ceramics owing to a metallic behaviours of HfC and $MoSi_2$. Comparing the two classes of samples, it is possible to conclude that higher $MoSi_2$ content decreases slightly material resistivity, inducing a positive electric effect.
2. **Silicon carbide-based samples** *(S, SAY, SAYM-30)*: in this case, materials resistivity depends largely on the content of the additives.
    - Pure SiC has a semi-conductor behaviour, although its resistivity is far smaller than that of intrinsic SiC (5×10^2 Ω cm against 10^9 Ω cm) owing to a defected structure, if compared to the single crystal.
    - SAY contains aluminium and yttrium oxide as additives, which act as electric insulators. The resulting resistivity is thus even higher than pure silicon carbide.
    - SAYM-30 has a not-negligible $MoSi_2$ concentration (30%) that results in a far lower resistivity compared to the other SiC-based materials, owing to percolative electric conduction mechanisms among $MoSi_2$ regions.
3. **Aluminium nitride-based samples** *(ASMY-30)*: although based on a wide-band gap semiconductor like AlN (typically characterized by very high resistivity), on a not-negligible percentage of SiC and on an insulator (yttrium oxide), ASMY-30 has a 30% content of $MoSi_2$, which allows a resistivity just below the maximum allowable value (5 Ω cm).

On the other hand, refractory metals (like W, Mo) and pyrolitic graphite are compliant with the requirements in terms of electric resistivity. However, a few words have to be spent about pyrolitic graphite: it has been preferred to highly-oriented pyrolitic graphite (HOPG) because its cost is more than two orders of magnitude lower than HOPG (about 300 €/cm^2 for 3 mm thick sheets) and it shows less anisotropic properties.

3.2.2 Integration of thermionic emitter on the absorber. CNR-IMIP

The thermionic emitter has been deposited directly on the absorber back surface, the one not exposed to solar radiation, aimed at a monolithic integration of the thermionic stage; in this way, the thermionic active material is able to form very stable physical bonds with the absorber material.

The most promising material for thermionic emission, developed within E^{2}PHEST^{2}US project, is polycrystalline diamond, a material grown by chemical vapour deposition methods (CVD) by CNR-IMIP. Two techniques have been exploited: hot-filament CVD (HF-CVD) and microwave CVD (MW-CVD). They have in common the gaseous reactant precursors and the thermodynamic growth parameters (methane and hydrogen as gases, substrate temperature from 700 to 800 °C, gas pressure from 15 to 40 Torr) while they differ in the energy source for gas activation (hot filament or microwave power, respectively). Each technique has its advantages and disadvantages, which are synthetically summarized in Table 4.

	Advantages	Disadvantages
MW-CVD	• Clean process • High deposition rates (0.5-5 μm/h) • Possibility of n-doping (nitrogen) • Hydrogen termination (in situ)	• Not uniform film thickness from centre to borders (bow).
HF-CVD	• Deposition of controlled and constant film thickness on large surfaces (up to 10 inches)	• Pre-carburizationtion of the filaments • Possible pollution from the hot filament material (Ta) • Lower deposition rates (0.1-1 μm/h)

Table 4. Advantages/disadvantages of HF-CVD and MW-CVD deposition techniques.

Preliminary experiments of CVD diamond deposition has been carried out on all ceramic samples by MW-CVD. The mechanical stability of diamond films on a specific substrate depends on the matching of its lattice constant and thermal expansion coefficient to the substrate. The first requirement (lattice) is responsible for the stability of the diamond chemical bonds on the substrate (i.e. adhesion); the second one is related to the film thermal stability at high temperature and during thermal cycles.

Scanning Electron Microscopy

Fig. 10 shows SEM micrographs of CVD diamond on ceramic samples. Analyzing Fig. 10a and b, there are negligible differences between the image obtained by secondary and backscattered electrons: this underlines very high compositional purity of the deposited material (carbon-content is very close to 100%). Fig. 10c shows a HCM-30 sample, on which diamond film has delaminated, leaving the HfC surface uncoated. The diamond film remains stable only on the disc edges, where the rounded geometry compensate the high film internal stresses (Fig. 10d).

The mean grain size of the diamond film is approximately constant for all the different substrates (it depends only on film thickness, and thickness is comparable). This is true except for ASMY-30 sample, where the diamond grain size is visibly smaller than the other cases (Fig.10g). This depends from the low deposition rates on nitrides.

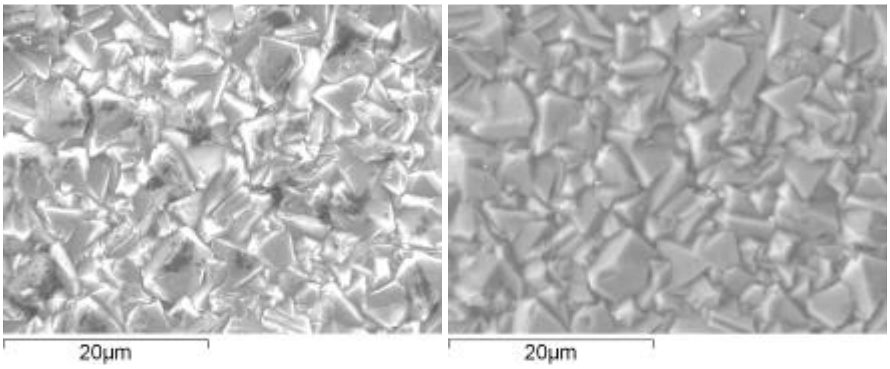

HCM-5: a) and b)

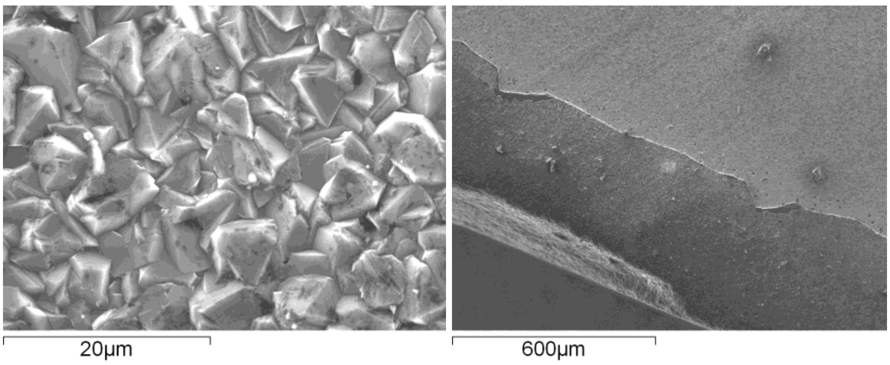

HCM-30: c) and d)

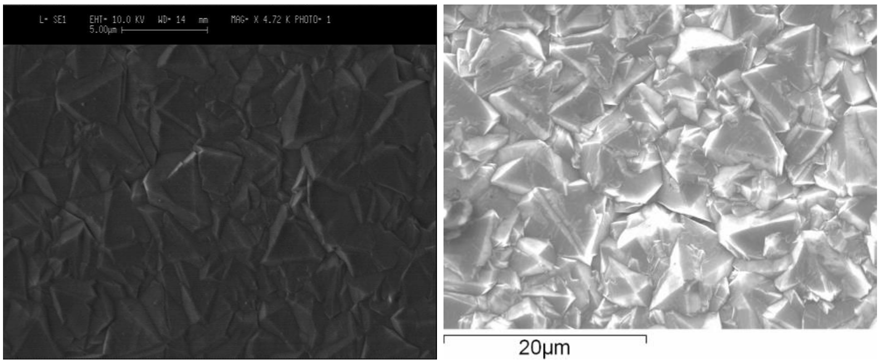

S: e) and SAY: f)

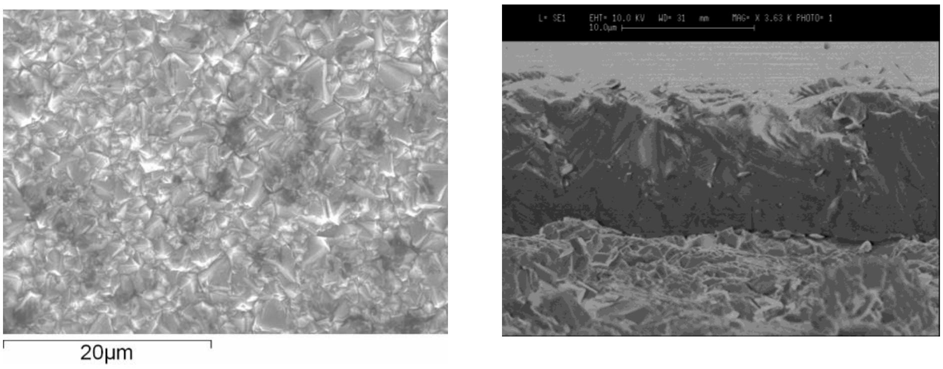

ASMY-30: g) and h)

Fig. 10. SEM micrographs of CVD diamond deposited on ceramic materials. Specifically, in a) the secondary electron emission detector and b) backscattered electron detector image of a diamond film on HCM-5. c) Image of HCM-30 sample with diamond film grown only on the disc edges (d). Diamond film on e) SiC sample, f) SAY, g-h) ASMY-30.

Raman Spectroscopy and XRD spectroscopy

Both Raman spectroscopy and XRD are fundamental analytic tools for the evaluation of the structural quality of the deposited CVD diamond films. From a detailed analysis, medium-high quality films can be obtained by using HCM-5, SAYM-30 and ASMY-30 substrates. Pure SiC is the substrate that guarantees the lowest internal strain, which increases by introducing other additives within the substrate (SAY and SAYM-30). Diamond films deposited on ASMY-30 and HCM-5 have comparable internal compressive strain.

.

Conclusions about CVD diamond depositions and possible alternatives

In Table 5, thermal expansion coefficients of substrates under investigation are reported. The CVD diamond thermal expansion coefficient is about 1×10^{-6} K^{-1}, that is lower than those of all the ceramic samples used as substrates On the other hand, diamond has demonstrated to have a very good lattice match with carbides and nitrides, but less with silicides.

The films have been successfully grown (thickness from 4 to 10μm) on all substrates but HCM-30, on which surface the films always underwent delamination, owing to strong internal stresses. The grown diamond films has demonstrated to be stable with temperature (as confirmed by repeated thermal cycles from room-temperature to 800 °C).

On the other hand, ASMY-30 and SAYM-30, with the same percentage of molybdenum silicide, proved their adhesion compatibility with diamond.

These indications suggested that molybdenum silicide is not a proper substrate for diamond deposition and its presence in high concentrations could induce increased stress on the growing diamond film. In case of substrates containing elements with a full compatibility to diamond (like silicon carbide and aluminium nitride), there is probably a mitigation of this effect.

These findings suggested to decrease the value of $MoSi_2$ in the ceramic samples.

Sample Name	**Material**	**Thermal expansion Coefficient**	**Compatibility with CVD Diamond**
HCM-5	HfC + 5% $MoSi_2$	6.6×10^{-6} K^{-1}	***
HCM-30	HfC + 30% $MoSi_2$	6.6×10^{-6} K^{-1}	-
S	SiC	6.6×10^{-6} K^{-1}	***
SAY	SiC + 6% Al_2O_3 + 4% Y_2O_3	4.95×10^{-6} K^{-1}	**
SAYM-30	(SiC + 6% Al_2O_3 + 4% Y_2O_3) + 30%vol $MoSi_2$	5.0×10^{-6} K^{-1}	***
ASMY-30	(55%vol AlN + 15vol% SiC + 30vol% $MoSi_2$) + 2wt% Y_2O_3	6.9×10^{-6} K^{-1}	***
W	W (99.999% purity)	4.5×10^{-6} K^{-1}	*
Mo	Mo (99.999% purity)	4.8×10^{-6} K^{-1}	*
C	Pyrolitic Graphite (99.999% purity)	4.3×10^{-6} K^{-1}	-

Table 5. Thermal expansion coefficient of ceramics and other materials used as substrates for diamond deposition and their compatibility to which has been assigned a mark (*) identifies the lowest value, while (***) the highest value, - no possible deposition).

Surface texturing by ultra-short fs laser treatment by CNR-IMIP Potenza

Aimed at reaching the goals of E²PHEST²US project, the Potenza branch of IMIP devoted its efforts on preliminary laser treatments of the absorbers' surface.The main goal of the surface treatment was to enhance the ceramic receiver surface absorbance in a wide range of wavelengths, mainly in the visible-near infrared regions.

After preliminary surface treatments on different materials, mainly carbides (SiC, HfC) and pure metals (W, Mo), the processes were optimized and adopted for the treatment of the ceramic discs (, 3.5 cm in diameter), aimed at obtaining a standard procedure for the maximum attainable increase of light absorbance. The parameters have been optimized as a function of material structure and initial surface roughness.

The parameters considered during the treatments were:

- laser pulse energy (in the range 0.2 – 2.0 mJ/pulse);
- spot focusing (diameter in the range 100 μm - 0.5 mm);
- speed of the translational X,Y stage under the laser beam (range 0.2 – 3.0 cm/s);
- acceleration of the translational stage under the laser beam (range 1 – 4 cm/s^2).

The laser wavelength (800 nm) was kept constant.

After the laser treatment, the following characterizations were performed: Scanning Electron Microscopy (SEM), Optical Microscopy, and UV-VIS-IR spectrometry using an integrating sphere.

The laser system employed (Fig. 13) is based on a Spectra Physics Tsunami S - fs oscillator (pulse duration about 100 fs, repetition rate 80 MHz, wavelength 800 nm, peak power > 0.7 W) pumped by a Spectra-Physics Millennia Pro 5sJS (CW, wavelength 532 nm, power 5W). The output of the oscillator is the seed for the Spectra-Physics Spitfire Pro 100 F 1K XP 4W amplifier (pulse duration < 120 fs, repetition rate up to 1000 Hz, wavelength 800 nm, pulse energy up to 4 mJ/pulse) pumped by a Spectra-Physics Empower 30 Q-switched DPSS (Diode Pumped Solid State) Nd:YLF (repetition rate 1000 Hz, wavelength 527 nm, pulse energy up to 20 mJ/pulse, pulse duration 100 ns).

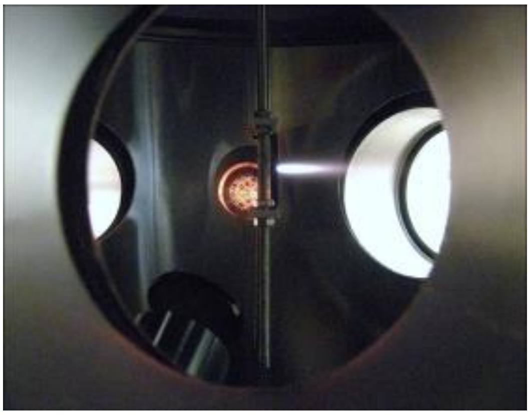

Fig. 13. Laser system employed for the treatments (*left*)**,** and inside view of the apparatus (*right*)

The absorbance measurements of the laser treated samples were performed using a black mask of absorbing material (minimum absorbance value of 97%) in order to isolate a square (10 mm x 10 mm) of the treated zone with respect to the surrounding surface.

The absorbance measurements were deduced from the reflectance measurements, neglecting the transmittance. In Fig. 14 some examples are reported, in which the absorbance of the treated samples has been compared to the untreated zones measured on the original samples.

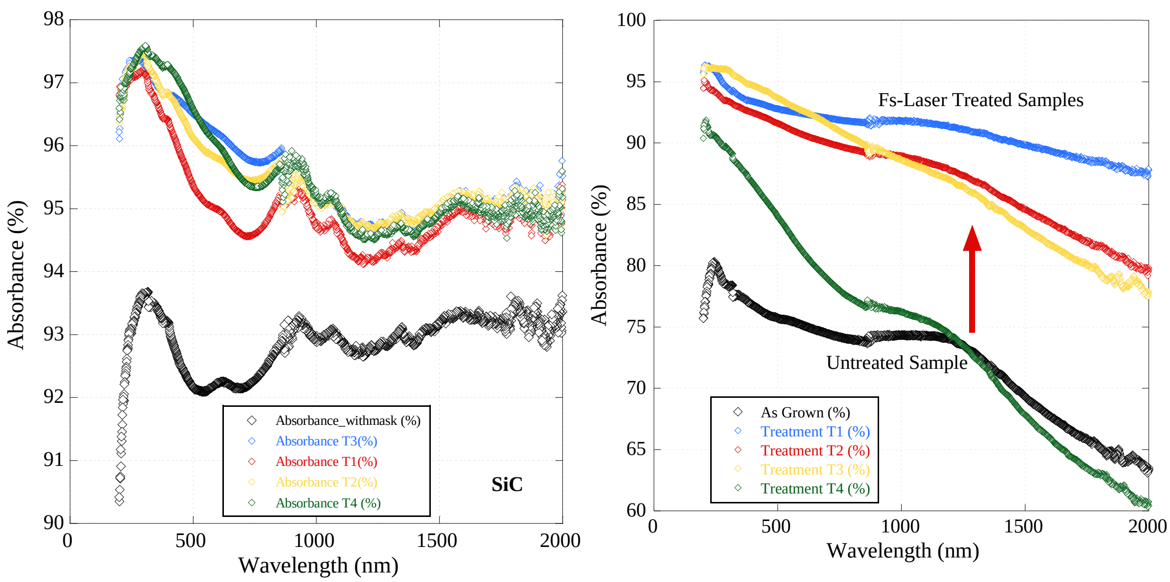

Fig. 14. Absorbance of differently treated zones of the SiC sample (left) and HCM30 sample (right). The black curve is the original surface absorbance. T# is the treatment number.

Fig. 15 reports the evaluation of the solar absorbance α for the treated samples as a function of the specific treatment. It is noticeable an increase in the absorption efficiency induced by the surface treatments, that quantitatively demonstrates the efficacy of the technique. The treatment induces efficiency values even higher than 90%. The differences between non-treated SiC and non-treated HfC were further reduced, limiting the material intrinsic properties, despite to diffraction effects.

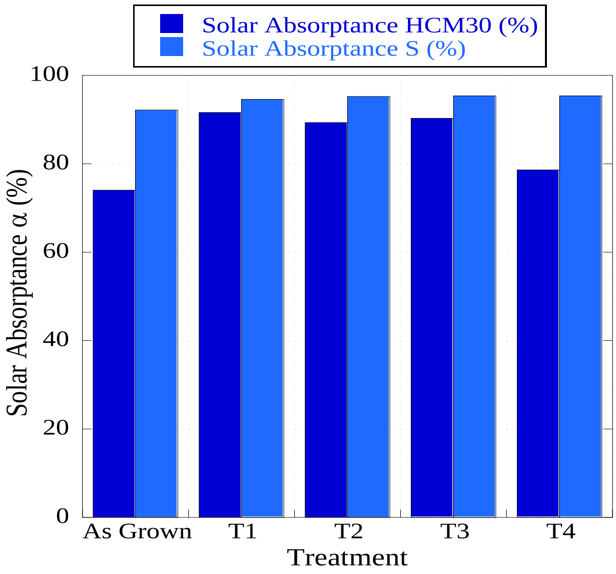

Fig. 15. Comparison of solar absorptance for the samples HCM30 and S**.**

Under the micro-structural point of view, Fig. 16 shows the evidence of micro-patterning of the surface, induced by the laser treatment. A periodic structure composed by lines distant about 800 nm (i.e. the laser wavelength) acts like a blazed diffractive grating that enables a more efficient capture of the impinging radiation.

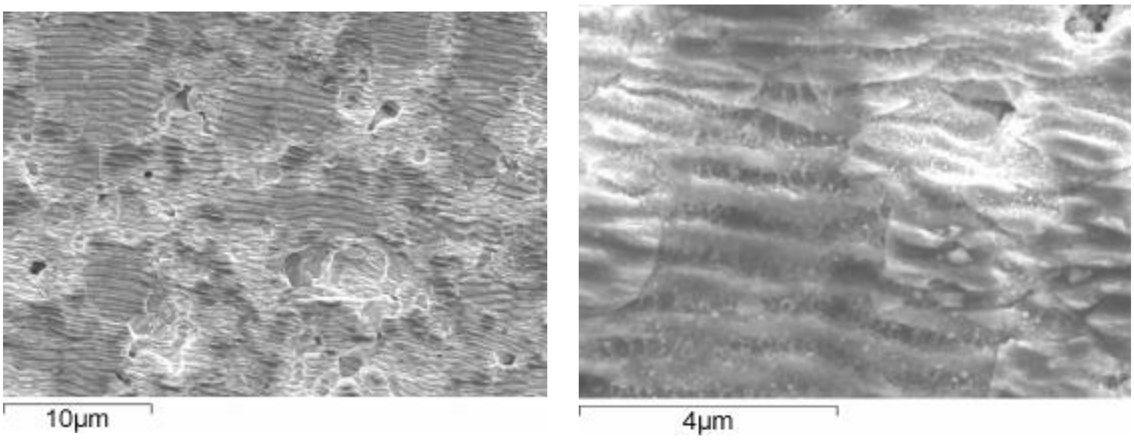

Fig. 16. Evidence of micro-patterning of the laser treated surface (HCM30 sample) by scanning electron microscopy (higher magnification on the right side).

The textured (or nano-structured) surfaces produce high solar absorbance by multiple reflections among needle-like, dendritic, or porous microstructure, like in the natural effect, well known as the Mott's eye effect, Fig. 17. Comparing the SEM images it appears very similar to the real effect on our laser treated solar receiver (Fig. 18).

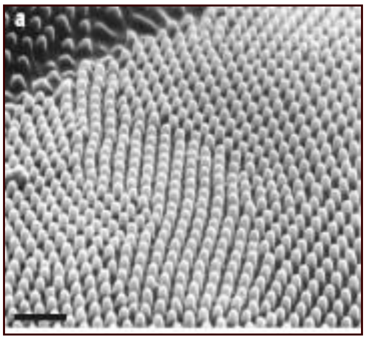

Fig. 17. SEM of the Mott eye

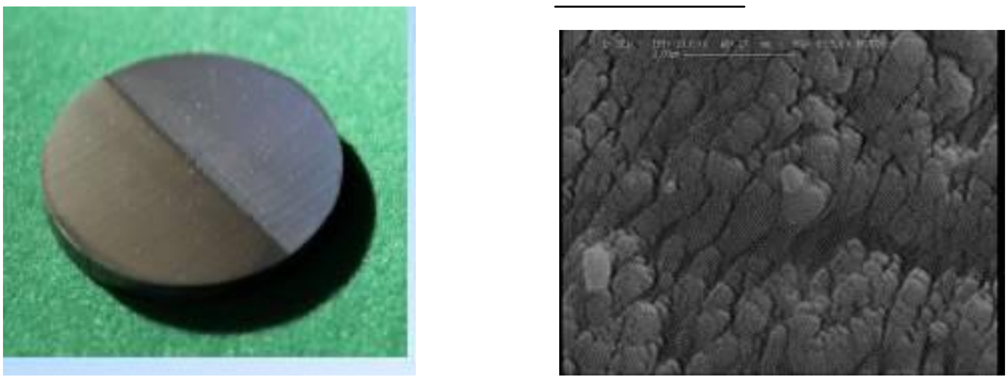

Fig. 18. The treated ceramic disc absorber (left) and the nano-textured surface (~200 nm) (right*)*

Thermal emittance

Fig. 19 reports the thermal emittance of all analyzed materials. The radiation emittance is a loss and should be as low as possible: under this point of view, refractory metals are the best choice (< 40%). Hafnium carbide based materials achieve an optimal emittance (about 50%), whereas silicon-carbide and aluminium-nitride based samples show high emittance values as well as pyrolitic graphite. Among the silicon carbide based materials, the SAYM-30 has the minimum thermal emittance. It is interesting to notice that the extracted values of emittance are in agreement with the total emissivity coefficient reported in literature for the main material component (e.g. HfC for HCM samples or SiC for SAYM ones).

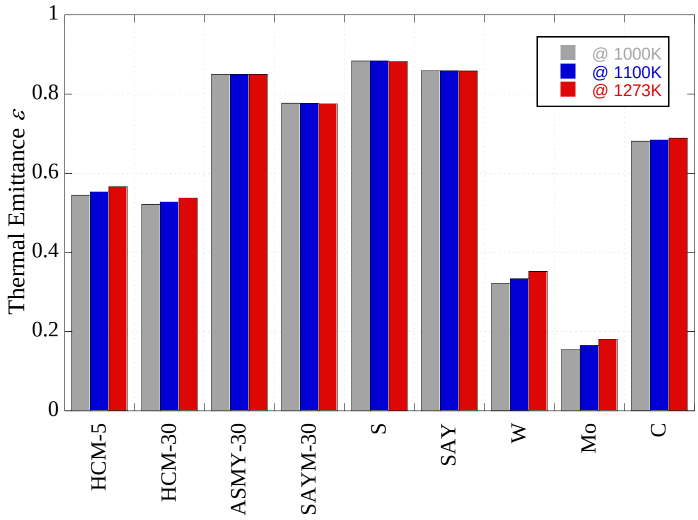

Fig. 19. Thermal emittance of the analyzed materials at 1000, 1100, 1273 K.

Conclusions on preliminary materials

We observed that each material reserves advantages and weak points with respect to the requirements established by the absorber application. Table 6 reports in the most important functionalities of the characterized materials, by assigning them an evaluation mark. The unacceptable values for the application are evidenced in red.

Specifically:

- HCM-30 can be eliminated, owing to its incompatibility with CVD diamond deposition and to its less appealing physical properties than HCM-5;
- S and SAY can be eliminated owing to their too high electric resistivity;
- W, Mo, and pyrolitic graphite proved their poor compatibility with CVD diamond.

The solar absorption efficiency parameter is less critical, since the femto-second laser texturing proved its capacity of improving the optical properties of the surfaces as a post-treatment. In other words, post surface texturing can have a key-role in compensating intermediate solar absorption efficiency showed by some materials (HCM-5, SAYM-30).

Thermal emittance characterization is not so critical, since the thermal loss can be prevented, in our configuration, by: 1) Depositing a thin layer of refractory metal on the absorber lateral surface; 2) Depositing a very thin layer of IR reflecting material on the optical window back surface.

As a preliminary conclusion, the experimentation was continued on HCM-5, ASMY, SAYM materials, which were chosen as possible candidates for the CM final development. ASMY and SAYM materials were successively developed by varying the molybdenum silicide content in order to make these materials more compliant to the application. This is discussed in the following paragraph.

Sample Name	Materials	Solar Absorption Efficiency	Electric Performance	Thermal emittance	Compatibility with CVD Diamond
HCM-5	HfC + 5% $MoSi_2$	**	***	**	***
HCM-30	HfC + 30% $MoSi_2$	*	***	**	-
S	SiC	***	*	*	***
SAY	SiC + 6% Al_2O_3 + 4% Y_2O_3	***	*	*	**
SAYM-30	(SiC + 6% Al_2O_3 + 4% Y_2O_3) + 30%vol $MoSi_2$	**	***	*	***
ASMY-30	(55%vol AlN + 15vol% SiC + 30vol% $MoSi_2$) + 2wt% Y_2O_3	***	**	*	***
W	W (99.999% purity)	*	***	***	*
Mo	Mo (99.999% purity)	*	***	***	*
C	Pyrolitic Graphite (99.999% purity)	**	***	*	-

Table 6. Evaluation marks for each material functionality for constituting the absorber ("*" identifies the lowest value, while "***" the highest value," –" means no possible evaluation**)**

3.2.3 Refinement of the Absorber Materials

Role of Molybdenum Silicide

All the ceramic materials proposed for the absorber contain molybdenum silicide, that has the role to stabilize their structure and reduce internal strains. The introduction of $MoSi_2$ has been demonstrated to induce:

1. A decrease in optical absorption;
2. A decrease in electric conductivity;
3. A lower compatibility to the CVD diamond deposition.

The content of $MoSi_2$ has to be reduced to a minimal value able to guarantee structural stability and an acceptable electric resistivity.

The second type of refined samples produced by CNR-ISTEC are resumed in Table 7. Together with a new set of HCM-5 samples, two sets of ASMY and SAYM samples with a

10%-reduced content of molybdenum silicide were produced. Moreover, in order to evaluate the possible application of borides, a temperature-resistant material as zirconium diboride with a 20% content of silicon carbide was fabricated.

Sample Name	Materials	Surface Roughness (μm)
HCM-5	95 HfC+5 MoSi2	0.10
SAYM-10	SiC + 10 MoSi2 + add.	0.03
ASMY-10	65 AlN+25 SiC+10 MoSi2 + add.	0.10
ZrB2 100*	ZrB2+ 20 SiC + add	0.10

Table 7 . Ceramic materials revised as a function of the preliminary characterization results.

Conclusions on the refined materials

Tab. 8 reports synthetically the quality marks for the refined materials:

- SAYM-10 has a solar absorption efficiency larger than SAYM-30, at the cost of a minor electric conductivity, which is in any case compliant with the requirements.
- ASMY-10, although shows higher absorption efficiency and compatibility with CVD diamond, has an unsatisfying electric performance. ASMY-30 has to be preferred to it.
- ZrB2. These samples show a very low resistivity, but they have a poor absorption efficiency and compatibility with CVD diamond.

Sample Name	Materials	Solar Absorption Efficiency	Electric Performance	Compatibility with CVD Diamond
SAYM-10	SiC + 10 MoSi2 + add.	***	**	***
ASMY-10	65 AlN+25 SiC+10 MoSi2 + add.	***	*	***
ZrB2	ZrB2+ 20 SiC + add	*	***	*

Table 8. Evaluation marks for each material functionality for constituting the absorber ("* identifies the lowest value, while "***" the highest value, "-" means no possible evaluation).

3.2.4 The Solar Test Platform construction at Castel Romano and the CM beta integration by SHAP and CNR

The main activities carried out for the designing and fabrication of Solar Test Platform (STP) have been focused on the study and the optimization of the parameters of the different systems involved (optical, mechanical and tracking) directed to realize an efficient concentrating solar system, able to provide the conversion module with a high amount of solar radiation power.

The different components have been designed according to the property features of the conversion module. The different subsystems (mechanical, optical and electrical systems) as well as the thermal circuit have been designed while the control system for all the apparatus management was tested and optimized. Overall evaluation of parabola focus, radiation flux concentration and maximum temperature reached at the focal point, where positioned the CM has been carried on. Special efforts have been dedicated for the construction and automatic control of the x,y,z step motor controlling systems necessary to integrate the CM into the Platform.

Fig. 20. the conversion module with the pumping system, the beta version, installed at the STP .

3.2.5 Hybrid cable achievements.

In the first 18 months of the project Prysmian has designed the hybrid cable, and tested materials and components suited for its production. In particular, the shape of the cable has been considered: circular sections are easiest to be produced and handled, however it was found by simulating several shapes that a flat structure could better dissipate heat generated by high current and hot water. This is due to a larger ratio between external surface and section area. The flat structures also enable to align the cable along the thinner side facing the concentrated radiation, limiting its shade.

Since the fluid circulating in the cable can be extremely hot due to slow reaction time of the control system, the tubes embedded in the cables should be heat resistant. Fluorurated materials were first adopted; however this solution is not compatible with smoke emission in case of fire. PEEK tubes were considered, and then dropped for their rigidity. Finally corrugated steel tubes were adopted as possible solution.

The simulation of the cable was completed; the cost calculated and send to production.

In the second half of the project the cable was produced and characterized according to the standards valid for photovoltaic cables. After the standard factory tests performed by Prysmian Germany, the cable was sent to Milan Prysmian headquarter R&D where it was completely re-characterized in order to match the simulation with the experimental tests. Electrical tests were performed with high voltage 1000 times higher than operating voltage, to highlight partial discharge (indication of poor homogeneity of the compound).

Bending properties of the cable were examined in detail, since in concentrating systems the cable is constantly moved and bent following sun tracker. In particular: a bending test machine was adapted to hold the flat cable, an optical fibre sensor was glued inside the tubes to monitor elongation and compression during the bending cycles. The bent cable simulation was compared with test results. Bending tests evidenced as a main failure mode the break of metal tubes welding; much effort has been dedicated to measure the quality of welding on metal tubes. Pulling test of cable and impact test have been performed, even if not relevant for the application unless in case of accident.

The cable structured has been described in a patent application devoted to solar concentrating generators.

Fire tests offered unexpected positive results in terms of flame propagation limitation. 6 fire tests were performed in different water filling conditions, and a general patent application (not limited to solar cable) has been filed. All the materials used in the cable have been tested with physical chemical methods. In particular DMTA, DSC and reometer have been used to study the coupling of the different compounds.

As one main source of failure of the cable there is a poor carbon black distribution in the sheath. First we studied UV damage of compound using cables taken from the field and also running dedicated laboratory tests; we found a carbon black threshold, and then we invented two non-destructive optical methods to detect carbon black comparable to TGA in terms of accuracy. At our best knowledge this measurement is possible with a non-destructive technique. Alternative compounds were tested to balance heat dissipation in the cable and UV protection, and flexibility. An X-ray single projection measurement was optimized to measure the gap between the cable elements, which guarantees a stable mechanical performance. This test has been proposed for standard flat cable production.

3.2.6 The vacuum encapsulation of CM, the preparation of gamma version and the integration at STP

The design is based on the idea to allocate the CM in a body flange shaped to be compatible with a standard ConFlat® flange, so as the device proves to be compact and very flexible; the module prototype is fasted on top by a commercial fused silica windowed flange. A copper heat sink is designed for quartz window cooling (not shown in CAD figures). This configuration allows to minimize optical losses, and to make it in the future commercially more attractive, reducing largely the device dimensions. In Fig. 21 a schematic draft of the body flange is shown.

Fig. 21. Three sides view of designed CM

Active part of conversion module has been redesigned in order to be less space-consuming (Fig. 22). The thermoelectric module is directly in contact with CM on cold pole, while hot pole is under the collector stage. Ferrule radius has been enlarged to host screws for fastening to the CM.

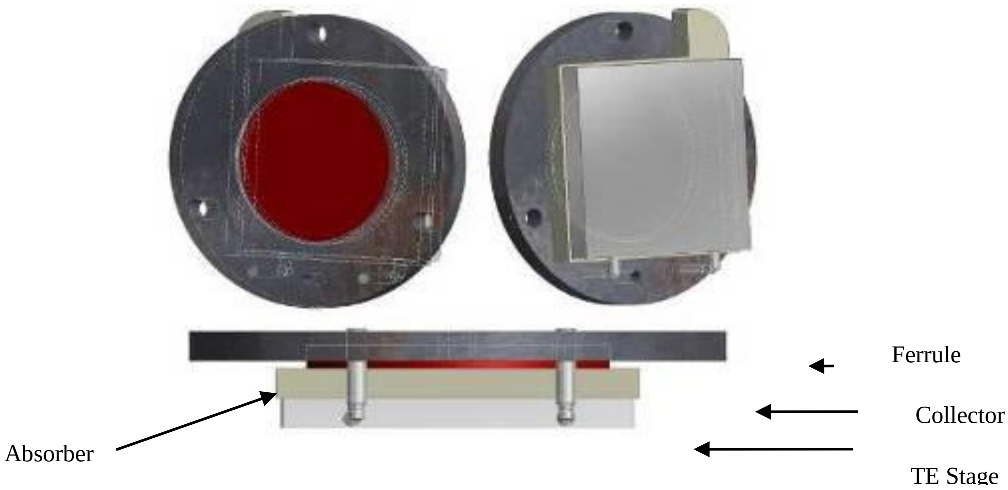

Fig. 22. Conversion module active stage

Fabrication and assembly

The various components (Copper heat sink, transparent windowed flange, stainless DN63CF body flange, Molybdenum ferrule, absorber/thermionic emitter, ring-shaped spacer, Molybdenum collector, thermoelectric module, getters) have been purchased or directly produced. After an electro-cleaning process, the conversion module body enclosure has been assembled and tested for vacuum operation with a leak detector. The conversion module enclosure keeps a vacuum better than 3×10^{-8} mbar×l/s.

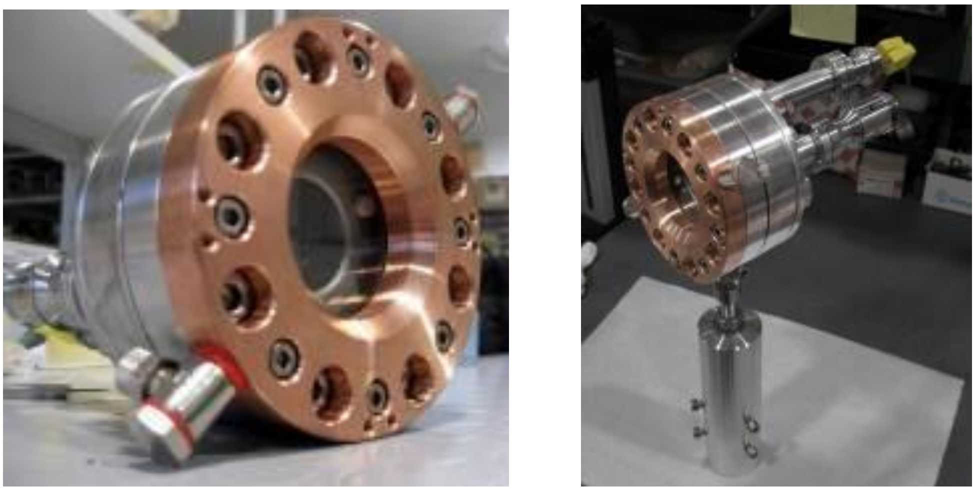

Fig. 23 – Front (*left*) and rear (*right*) view of assembled encapsulated Conversion Module

Fig. 23 shows the encapsulated CM. This configuration has been also tested for vacuum operation; the encapsulated conversion module keeps a vacuum higher than 10^{-8} mbar×l/s .

3.2.7 Integration of CM (Gamma) with STP

Assembled encapsulated CM has been mounted on STP, ready for conversion operation. Four calorimeters are mounted at an angle of 90° with one another, to control the concentrated solar spot position, respect to the view-port. Measurements have been performed and are ongoing for the coming days. It is remarkable to notice that vacuum level results stable around 2×10^{-6} mbar. In the following, pictures of encapsulated CM installed at STP.

Fig. 24– CM (Gamma) integrated in STPat the focal point of the parabola (rear view)

3.2.8 The lab tests on naked CM by solar simulator at TAU

The lab test at TAU have been performed on naked CM (shown mounted within the system in Fig.26), located into a vacuum chamber, so as to act in the optimal conditions to make the test on the thermionic and thermoelectric emission properties, under controlled conditions of vacuum and concentration of radiant flux, obtained in the solar simulator show in the Fig. 25.

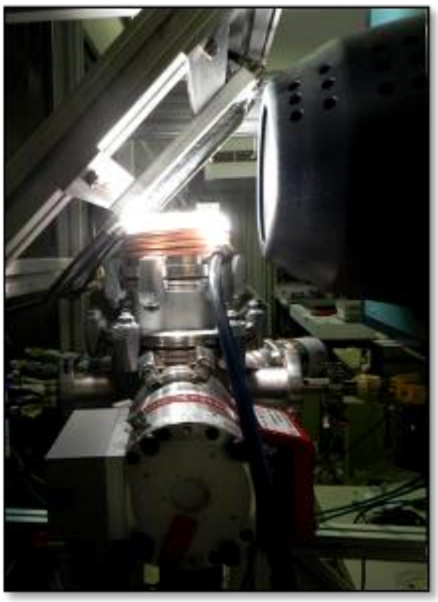

Fig.25 The solar simulator at TAU

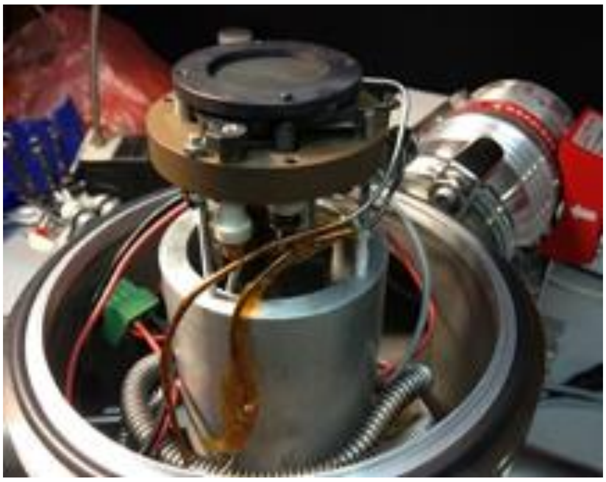

Figure 26. CM-Alpha

The efficiency of the system, both power and electricity, is strictly related to the temperature of the emitter, as shown in Fig. 27, but also to the vacuum level inside the chamber Fig. 28.

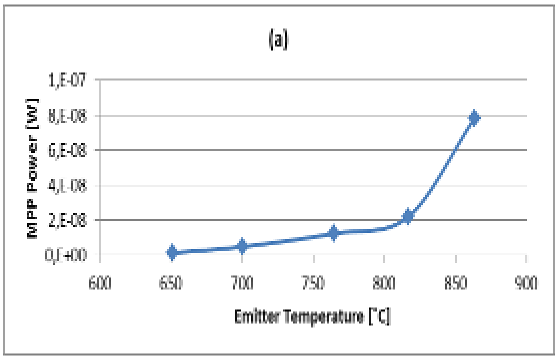

Fig. 27. Thermionic power vs. emitter temperature

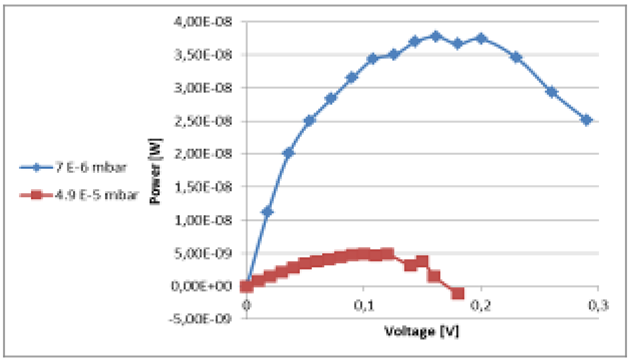

Fig . 28 Thermionic power vs. vacuum conditions

Fig. 29 shows the dependence of measured current from the vacuum level inside the chamber.

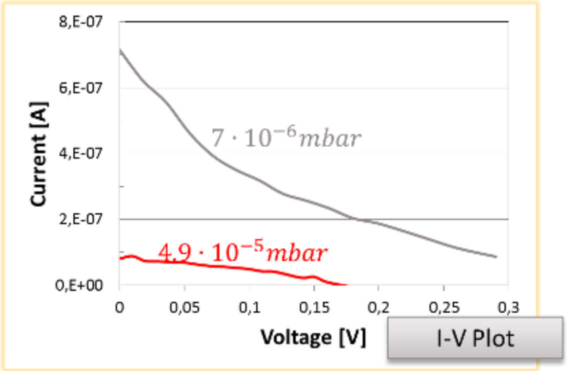

Fig. 29. I-V plot as function of different vacuum level inside the test chamber.

Under STP, the CM shows a similar behaviour to that found under solar simulator. The CM total output power practically superimposes the TE stage output power owing to a low contribution of the TI stage. It is possible to evaluate the conversion efficiency by dividing the total output power by the input one as a function of TI emitter temperature. The data are shown in Fig. 30, where an increasing conversion efficiency dependence on temperature is evident. At 535 °C the total conversion efficiency is about 0.2%, while the thermal-to-electric one equal to about 0.4%. The thermal-to-electric conversion efficiency has been derived by considering that absorber thermal emittance is about 50%, thus 50% is approximately the energy lost by the absorber and not transferred to the TI emitter.

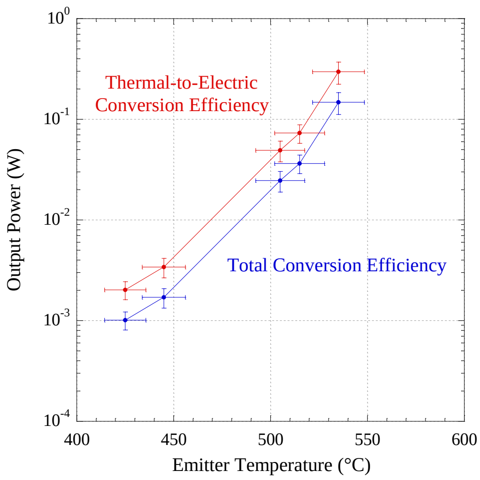

Fig. 30. Total conversion efficiency and thermal-to-electric conversion efficiency as a function of emitter temperature.

Thermal efficiency of our system is (58% ± 1%). It means that about 58% of the radiation power that reaches the CM is converted into thermal power. This latter heats the coolant that passes through the CM in its front and rear parts.

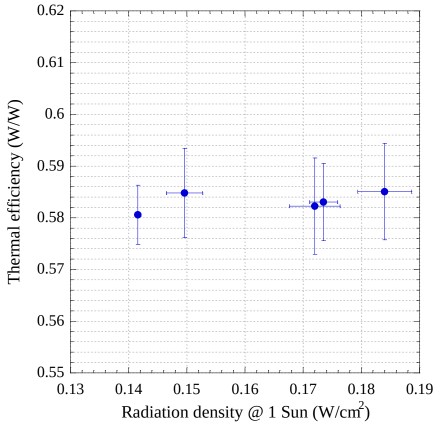

Fig. 31. CM thermal efficiency as a function of the illumination level at 1 sun.

3.3 Conclusion

Coming to S&T conclusion, the values of both power and current are not satisfactory. Their values are low compared to prediction. Their strict dependence from vacuum level and receiver temperature are well known in the thermionic process. In this Conversion Module, in addition, many parameters are very sensitive and difficult to control and optimize, since we are dealing with a complex prototype system, with many components, all difficult to control properly, both as regards the vacuum maintenance, under operative conditions, both for other properties more strictly linked to the performance of the innovative materials, in particular, absorption of light, texture, stability of the coatings (adhesion), stable H-terminated diamond (thermionic emitter material), appropriate work function difference between the cathode and anode, various sealing components and electric pass-through, in addition to the low level of temperature reached by the absorber.

Solutions require further research/optimization, of both fundamental and technological type, to the extent that you want to achieve substantial improvements of the whole system.

- Improve material properties and related treatments (complex ceramic receiver, surface nano-texturing, diamond quality, doping and H-termination, adhesion, higher difference of work function (anode-cathode) by cesium treatment of Mo surface, minimizing inter-electrode distance, better quality commercial thermoelectric components.
- Strive to reach the maximum obtainable value of vacuum controlling the whole system, undesired outgassing under heating, optimum sealing materials, getters quality.
- Introduce mechanical spacers to reduce gap width, avoiding space charge-effects
- The energy fluence at the STP should be verified during the summer season, in order to have a better weather stability and a more reliable statistical analysis, and some STP components, which are not working optimally, possibly substituted.

4 The potential impact and the main dissemination activities and exploitation of results

From a technological point of view, the main impacts of E^2PHEST^2US project are:

- direct conversion of solar power to electrical energy;
- coupling and exploitation of two physical phenomena such as thermoelectric and thermionic emission, coupled in series, to produce electricity from concentrated solar radiation
- development of innovative high temperature solar-radiation absorbing, thermionic materials (complex high refractory ceramics and n-doped CVD diamond coatings) with possible benefits in other R&D fields, mainly high-temperature industrial applications;
- surface nano-structuring of solar radiation ceramic receiver , by means of an ultra-short fs- laser treatments, highly improving solar radiation absorption , minimizing light reflection
- newly devised method for vacuum encapsulation of a complex geometry (the CM) system
- newly designed high flexible hybrid cable for fluid and electric transports
- electrical conversion efficiency of the module potentially higher than standard PV semiconductors or equal to the multi-junction-based PV modules;
- high working temperature values and high conversion performance, unlike in semiconductor PV systems, severely damaged above 400 °C;
- easy-to-handle system, totally scalable in dimensions, modular, and potentially integrated in different high efficiency solar concentrating apparatuses (dishes, Fresnel lenses, parabolic mirrors, etc.);
- a system easy to be installed on roof-tops or facades of rural isolated houses or on city buildings;
- no need for extensive areas of installation (like CSP towers or parabolic through);
- no need of fused salt for heat transportation, nor of cooling water with a very low environmental impact;
- a technology that can be potentially transferred to solar space applications, or to other thermal energy recovery applications for high temperature process industry, automotive, aerospace (furnaces, engines, etc.).

Generally, E^2PHEST^2US project is expected to generate also the following impacts:

- energy saving benefit from the reduction in consumption of fossil fuel, directly translated into monetary benefits;

- reduction of environmental pollution. This technology replaces oil consumption and contributes to "*reducing greenhouse gases and pollutant emissions*," according to the EU policy towards the Kyoto protocols. Conventional energy generation and transmission methods can damage air, climate, water, land and wildlife landscape, as well as raise the levels of harmful radiation;
- at the end-user site, an additional benefit of reducing fuel transportation and electricity transmission losses;

Within the project it has been shown that given materials with the required properties, the theoretical conversion efficiency can reach up to 30%, and even higher with a secondary stage that uses the waste heat from the primary stage. This concept of a thermionic/thermoelectric solar converter has therefore the potential to compete with the more traditional CSP thermo-mechanical converters, while offering unprecedented scalability and flexibility.

The development of an effective solid-state solar converter for high temperature operation is primarily a challenge in materials. The development of critical elements in the thermionic converter has been presented, with first demonstrated achievements: cathode materials offering stability at high temperatures, surface treatment to increase radiation absorption, and emitter coating to increase electron emission at temperatures lower than conventional thermionic emitters. Further improvements are needed, as demonstrated by the preliminary tests that showed performance well below the theoretical predictions. On-going work includes mainly the continuing improvement of the emitter coating, by fine-tuning of the deposition conditions and film composition.

In parallel to the improvement of the primary stage, more performing thermoelectric generators are going to be commercially available and may be applied to improve the secondary stage. Even higher efficiency in thermoelectric converters is expected in the near future, with the development of nano-structured materials having a figure of merit $ZT > 2$. Therefore, the secondary stage contribution is expected to improve over the next few years.

Currently, the novel thermionic/thermoelectric is undergoing final tests under concentrated radiation, both in a controlled environment of a high-flux solar simulator, and under real sunlight concentrated by a solar furnace. The results of these tests will help in better understanding the characteristics and performance of the proposed concept, and in developing further improvements not only for the materials but also for the converter design and method of operation.

The main dissemination activities carried out by E^2PHEST^2US consortium aim to deliver the proper technical or business information to the right target. Conferences, scientific article, exhibitions and technical magazines have been the main tools used to disseminate information about the project.

Three speeches in three different Conferences[1] were published. Moreover, during the project lifetime a communication article has been published in the autumn edition of European Energy Innovation (September 2012). The issue contained a special report on SOLAR energy such as concentrated solar power (CSP), and photovoltaics (CPV). This special edition has been distributed to delegates attending the 27th European Photovoltaic Solar Energy Conference and Exhibition in Frankfurt on 25-28 September 2012. The magazine has also been distributed by name to MEPs and members of the European Commission, Energy and Environment Ministers in all 27 member countries, as well as Europe's leading energy companies and research institutes. This represents an estimated 16,000 readership.

In November 2012 it has been held in Antalya the E^2PHEST^2US Workshop, as part of a bigger event that has taken place in Turkey: SolarTR2 International Conference. Each project team member made scientific and/or technical presentation about the project and their contribution to the project. The consortium got also a stand in the exhibition where all the materials prepared to date were available and the project poster was posted at a number of locations in the hotel. Both the project booklet and leaflet were distributed, the E^2PHEST^2US Posters and a pair of promotional banners, realized for the event, decorated the stand. The E^2PHEST^2US Cable mock-up was on display at the booth as well. An up-to-date press release was also prepared and issued two weeks in advance.

Concerning the so-called printed materials, the following items have been realized:

- A leaflet;
- A booklet;
- A poster.

The leaflet has thought and developed to address principally the industrial audience. Indeed, all its features reflect mainly a market oriented approach, aiming to be attractive avoiding a too technical-scientific language. Its main goal is to spread the awareness about the existence of the project and give a quick insight about the partners. The leaflet was first distributed at SolarTR-2 International Conference and Exhibition.

Initially the booklet was thought as a follow up, enriched with further details and more technical information, of the leaflet. Instead during the project meeting held in Rome in July

---

[1] ***Thermionic Emission: A Different Path to Solar Thermal Electricity*** - By A.Kribus, D.M.Trucchi, A.Bellucci, E.Cappelli, P.Calvani, S.Orlando, D.Sciti, R.Yogev, Presented at SolarPACES 2012

Advanced Thermionic and Thermoelectric Conversion Module for Concentrating Solar Systems - By D.M.Trucchi On behalf of Ephestus Consortium, Presented at SuNEC 2012

Conversion Module for Solar Concentrating Systems (pg15) By CNR-IMIP team On behalf of Ephestus Consortium, Presented at Nanoforum 2012

2012 the partners opted to focus the booklet towards a more scientific content. Actually it has been agreed that the booklet that has been distributed at the project info day, gathers all the main scientific results achieved.

Besides the fact that the tool is more oriented towards the academic world, a key section is dedicated to clarify both the status of the E^2PHEST^2US development and the ownership of the results in order to allow potential investors to evaluate a potential business.

Moreover an A0 size poster has been designed for the SolarTR2 Conference in Antalya Turkey. The poster included the themes of ancient Rome as well as solar rays concentrated on an object representing the Conversion Module. Information about the workshop date and venue, as well as the project sponsor and partners were included in the poster.

Three patents proceedings have been finalized within E^2PHEST^2US project:

1. Thermionic converter device

Sept. 3rd, 2012 by: Trucchi, D. M., Cappelli, E, Sciti, D. and Orlando, S.

2. Combined dual-electrical and thermal cable

Nov., 2012 by: Sarchi, D. et al, PRYSMIAN

3. Cavo elettrico per un impianto solare per la generazione di energia elettrica e di energia termica ed impianto che lo comprende

Nov., 2012 by: Sarchi, D. et al, PRYSMIAN

The main exploitable results refer to the technological applications for STP – Solar Test Platform and CM – Conversion Module.

The software of the tracking system developed and finalized is applicable also to other different heliostats; in fact this system is able to follow the sun and to position the heliostat in the correct position to have the maximum concentration on a target. The mechanical movement of the heliostat utilizes actuators whose production costs are very interesting also for pre- series applications with fields of several heliostats with a single target.

For what concerns the CM in the actual configuration as designed during the development of the project, it needs further development to be applicable in concentrated solar power plants for distributed industrial and civil cogeneration.

Moreover, it can be applied in power generation system for energy recovery from hot gasses and heat furnaces deriving from continuous and intermittent industrial processes. For what concerns the device in a reduced configuration (only thermionic stage), it can be used in power generation as partial top cycle of a power unit fed with solid fuel (e.g. coal or municipal waste).

5 Contact details

The address of the project public website is: www.ephestus.eu

Project Co-ordinator contact details: Manuela Bistolfi

Consorzio Roma Ricerche

C/o Tecnopolo Tiburtino

Via Giacomo Peroni, 130

00131 Rome - Italy

Tel.: +39.06.40400134/137

Fax: +39.06.41294723

e-mail: innovation@romaricerche.it

Scientific Co-ordinator contact details: Emilia Cappelli

Consiglio Nazionale della Ricerca

Inst. IMIP

Via Salaria, km 29.3

00015 Monterotondo Scalo (Roma) -Italy

Tel: +39.06.9067 2230

Fax +39.06.90672 238

e-mail: emilia.cappelli@imip.cnr.it